



REVISTA INGENIO

Development of Oat Husk-Derived Nano-Silica for High-Performance and Sustainable Mortar Applications

Desarrollo de Nanosílice Derivada de Cáscara de Avena para Aplicaciones de Mortero Sostenibles y de Alto Rendimiento

Mohammadfarid Alvansazyazdi | Universitat Politècnica de Valencia - Spain
Alvaro Yerandi Carlosama Carde | Universidad Central del Ecuador- Ecuador
Jorge David Rosillo Pilamunga | Universidad Central del Ecuador- Ecuador
Pablo Mauricio Bonilla Valladares | Universidad Central del Ecuador- Ecuador
Debut Alexis Patrice Martial | Universidad de las Fuerzas Armadas - Ecuador
Jorge Luis Santamaria Carrera | Universidad Central del Ecuador- Ecuador
Hugo Alexander Cadena Perugachi | Universidad Central del Ecuador- Ecuador
Andrea Estefania Logacho Morales | Universidad Central del Ecuador- Ecuador
Jhon Fabricio Tapia Vargas | Constructora COVEVIM T&T S.A. - Ecuador

Recibido: 29/4/2025

Recibido tras revisión: 19/5/2025

Aceptado: 6/6/2025

Publicado: 10/7/2025

KEY WORDS

Nano-silica, oat husk, sol-gel, mortar, mechanical properties, plastering.

PALABRAS CLAVE

Nano-sílice, cáscara de avena, sol-gel, mortero, propiedades mecánicas, enlucido.

ABSTRACT

This study investigates the incorporation of nano-silica synthesized from agro-industrial waste—specifically oat husks—into plastering mortars. Amorphous silica is extracted through chemical treatment and converted into nano-silica via a sol-gel process, yielding 2.79%. Characterization through EDS, SEM, TEM, and XRD confirms nanoscale silica formation. Mortars are formulated using Atena Máster type N cement and fine aggregates from the “Copeta” quarry, verified under NTE INEN 2 536 standards. Nano-silica is added at dosages of 0.25%, 0.50%, 0.75%, and 1.00% by cement weight. The mixtures are evaluated in both fresh and hardened states. Fresh-state tests assess workability and flow, while compressive strength is measured at 7, 14, and 28 days. Results show that 0.25% nano-silica provides optimal performance, achieving 12.6 MPa at 28 days. Higher dosages lead to strength reduction, indicating a performance threshold. A cost-benefit analysis highlights the economic and environmental viability of converting agro-waste into high-performance materials. The findings underline nano-silica’s potential to enhance mechanical properties while promoting sustainability. This research demonstrates that controlled use of nano-silica from waste sources offers an eco-friendly, efficient solution for improving plaster mortar in the construction industry.

RESUMEN

Este estudio investiga la incorporación de nano-sílice sintetizada a partir de residuos agroindustriales—específicamente cáscaras de avena—en morteros para enlucido. La sílice amorfa se extrae mediante un tratamiento químico y se convierte en nano-sílice mediante un proceso sol-gel, obteniéndose un rendimiento del 2,79%. La caracterización mediante EDS, SEM, TEM y DRX confirma la formación de sílice a escala nanométrica. Los morteros se formulan utilizando cemento Atena Máster Tipo N y agregados finos provenientes de la cantera “Copeta”, verificados conforme a la norma NTE INEN 2536. La nano-sílice se incorpora en proporciones de 0,25 %, 0,50 %, 0,75 % y 1,00 % en peso respecto al cemento. Las mezclas se evalúan en estado fresco y endurecido. Las pruebas en estado fresco analizan la trabajabilidad y la fluidez, mientras que la resistencia a la compresión se mide a los 7, 14 y 28 días. Los resultados muestran que la adición del 0,25 % de nano-sílice proporciona el mejor desempeño, alcanzando 12,6 MPa a los 28 días. Dosificaciones superiores provocan una disminución en la resistencia, lo que indica un umbral de rendimiento. Un análisis costo-beneficio resalta la viabilidad económica y ambiental de convertir residuos agroindustriales en materiales de alto desempeño. Los hallazgos subrayan el potencial de la nano-sílice para mejorar las propiedades mecánicas de los morteros, al tiempo que promueven la sostenibilidad. Esta investigación demuestra que el uso controlado de nano-sílice proveniente de fuentes residuales constituye una solución ecológica y eficiente para mejorar el mortero de enlucido en la industria de la construcción.

1. INTRODUCTION

Mortar has been a fundamental component in societal development for decades, playing a crucial role in the advancement of civilization. As noted by Salamanca Rodrigo [1], the first mortar was made from stones and mud, later evolving to clay-based mixtures. By the 19th century, lime and sand were commonly used. Mortar is considered a specialized concrete mixture due to its similar composition, albeit with fine aggregate.

Currently, structural mortar has high demand due to its diverse applications, such as masonry bonding and plastering. There are standards that outline specifications for mortar preparation in construction; however, they do not specify on-site tests to determine its strength [2].

The search for innovative materials in the construction sector not only depends on advances in nanomaterials but also on the efficient management of experimental data and systematic analysis, as demonstrated through the application of executive dashboards for project monitoring [3].

In recent years, construction has undergone significant changes due to the emergence of nanotechnology. Materials have evolved into “super materials,” reducing environmental impact while enhancing their molecular structure to become lighter, stronger, self-adaptive, and intelligent [4]. These materials are modified at a scale of 1 to 100 nanometers, influencing physical, chemical, and biological reactions to reinforce the polymer matrix and regulate the controlled release of additives or active agents with antimicrobial properties [5].

The successful implementation of disruptive technologies, such as the incorporation of rice husk-based nano-silica, largely depends on organizational agility and the ability to rapidly adapt to emerging synthesis and characterization methodologies [6].

Just as the integration of information and communication technologies (ICTs) has transformed education methodologies, the incorporation of locally synthesized nano-silica into mortars represents a crucial step towards a more sustainable and innovative construction industry [7].

Among all nanomaterials, nano-silica has garnered significant attention from the construction industry. This is due to its superior pozzolanic activity, surpassing that of silica fume due to its larger specific surface area. This component reacts more efficiently with calcium hydroxide (portlandite), which is responsible for producing C-S-H gel, leading to enhanced early-age mechanical strength [8].

Given the high acceptance and interest shown by construction researchers, this study aims to analyze the characteristics that emerge when incorporating nano-silica into the mortar matrix. To achieve this, comparisons will be made with conventional mortar using standard materials such as cement, water, and fine aggregate. By the end of the study, the efficiency of nano-silica

incorporation will be evaluated in terms of compressive strength and permeability improvements.

1.1. SILICA MORTARS AND NANOPARTICLES

1.1.1. MORTARS

Definition and types of mortars

Mortar in the construction sector is defined as the combination of three main materials: cement or any binder, fine aggregate, and water. Often, it is necessary to add an admixture to the mix in order to improve certain properties of the mortar. Upon setting, the mixture exhibits behavior similar to that of concrete.

The NTE INEN 2518 standard describes five types of mortar based on the classification presented by the ASTM C-270 standard, with each type of mortar exhibiting its own characteristics, as outlined below.

Type M Mortar: It is characterized by greater durability compared to other types of mortars. It is used in structures that support heavy loads or are in contact with the ground or water.

Type S Mortar: Its main characteristic is adhesion to construction materials, such as in tile coatings for floors and walls.

Type N Mortar: It has medium strength, making it very useful as a binder for masonry blocks and wall coatings.

Type O Mortar: It has excellent workability but low strength. It is recommended for use in non-load-bearing walls of buildings with a maximum of two stories and coatings that are not exposed to harsh weather conditions.

Importance of Mortar in Construction

Mortars have various applications in construction, both in structural elements, such as in masonry buildings where this binder serves to support loads, and in non-structural elements. The most common use in our context is for non-structural elements, such as adhesives or coatings [9].

Mortar contributes in various ways to the preservation of a structure, such as in the use of mortars for waterproofing, thereby preventing damage to structural elements that could compromise the safety of the building. Similarly, mortar ensures the bonding of elements like blocks used in walls that divide different spaces, acting as a thermal and acoustic insulator to provide comfort for building occupants.

The aesthetic aspect of a construction largely depends on the final finishes, which are achieved with mortars to

eliminate imperfections or provide a specific style both inside and outside the building.

Improving mortar can aid in the evaluation of the seismic behavior of special moment frames using nonlinear incremental dynamic analysis [10].

Composition and Properties of Conventional Mortar

Mortar, like any construction material, possesses chemical, physical, and mechanical properties that vary according to the specific needs of the construction project. These properties are considered from the design of the mix to its preparation process.

Composition mortar

To prepare mortar, a binder, fine aggregate, and water are required. In some cases, special additives or aggregates may be used to enhance certain properties.

Properties of Mortar in the Fresh State

In their plastic state, mortars display a range of key properties that are crucial for assessing their behavior and effectiveness during fabrication and application in construction. Among these properties, workability and consistency are essential to ensure ease of handling and uniform application, thereby guaranteeing the quality of the construction work. [11]

Flow

This property is measured in the laboratory. The procedure involves placing the mortar in the form of a truncated cone on a vibrating table, then measuring the percentage increase in diameter after allowing the mortar to fall 25 times within 15 seconds from a height of 12.7 mm. [9]

Masonry units absorb a certain percentage of water, so it is recommended to maintain a workability range between 130% and 150% to counteract this absorption. [12]

Water Retention

The water retention capacity of mortar is essential to ensure that workers have sufficient time to adjust masonry units before the mortar hardens. [13]

Water retention capacity can be increased through various techniques, such as increasing the binder content, adding fine sand, or using water-retaining materials. [2]

Workability

This property is crucial in the mortar application process, as good workability facilitates the worker's task and ensures proper positioning of the masonry, while also preventing potential voids at the joints. Additionally, in

vertical plastering, the mortar provides good adhesion and uniform distribution for a better finish. [2]

Hardening

The hardening of mortar is directly related to workability. As the mortar loses water, its workability decreases, which could be detrimental. This hardening rate can be modified through the use of additives or techniques such as adjusting the temperature during the setting process.

1.1.2. Properties of Mortar in the Hardened State

Compressive Strength

One of the fundamental properties is compressive strength, which is influenced by three main factors. The first factor is the cement-to-sand ratio, where having a higher amount of cement relative to sand will exponentially increase the strength. The second factor indicates that mortars with a high fineness modulus exhibit greater strength. Lastly, it has been established that plastic mixtures perform better under compression than fluid mixtures. [14]

Absorption

The ability of mortars to absorb and retain liquids is a key factor in their strength and durability. High absorption can increase vulnerability to water infiltration, which could deteriorate structures and promote the appearance of cracks, corrosion of steel reinforcement. [15]

Permeability

Permeability in mortars refers to their ability to allow the passage of liquids or gases. A highly permeable mortar facilitates the infiltration of water and other substances, which can lead to moisture, structural corrosion, and the deterioration of building materials. Various factors influence this characteristic, such as poor mixing of components, application errors, or the use of inadequate or deteriorated materials. The presence of permeable mortars increases the risk of damage in areas where they have been used. [16]

1.2. NANOTECHNOLOGY AND NANOMATERIALS.

Nanotechnology emerged in the latter decades of the 20th century, driven by the development of new enabling technologies for imaging, manipulating, and simulating matter at the atomic scale [17]. This field involves controlling matter at the nanoscale and exploiting novel phenomena and properties, often by combining nanotechnology with other study areas like supramolecular chemistry [18]. By reducing material dimensions to the

nanometer scale, particularly below 100 nanometers, quantum effects become prominent, significantly altering their physical, chemical, and electronic properties [19]. The application of nanotechnology can modify certain properties of concrete [20]. Nanomaterials are unique as they provide a high surface-to-volume ratio, representing the engineering of useful and functional objects at the molecular or atomic scale [21]. Nanomaterials are classified into four main categories. Among these, 0-D materials, such as Au and Ag nanoparticles and fullerenes, exhibit all their dimensions at the nanoscale. Meanwhile, 1-D and 2-D materials, such as carbon nanotubes and graphene, respectively, have one or two dimensions smaller than 100 nm. These latter materials are widely used in industries such as pharmaceuticals and electrical adhesives [22].

1.3. SILICA NANOPARTICLES

Background

Silica nanoparticles have gained widespread acceptance and recognition worldwide due to their diverse physico-chemical properties. Based on particle size, mesoporous silica, ranging from 2 to 50 nm, exhibits enhanced adsorption/absorption behavior for hydrocarbons and can adsorb large molecules such as proteins [23]. In contrast, nanoporous silica particles, which are smaller than 2 nm, have the ability to absorb gas molecules [24]. Additionally, this material emerges as an alternative to microsilica, which is produced through the reaction of silicon at high temperatures [25]. The incorporation of nano-silica enhances performance and durability, contributing to the reuse of alternative materials and by-products from industrial processes, thereby generating a direct environmental benefit [26]. It is important to note that when using this nano-addition, cement demand decreases, while water demand in the mix increases due to its high specific surface area [6].

The use of agro-industrial waste, such as oat husks, for the synthesis of nano-silica offers a sustainable alternative that reduces environmental impact and promotes circular economy practices in the construction sector [27].

The various investigations take into account different sustainability problems in materials used in construction which can be improved, having several materials from which to choose, taking into account that the most important thing is to preserve the environment in order to preserve our planet [28].

Characteristics

Silica nanoparticles are spherical and exhibit pozzolanic activity. In mortars, they enhance dispersion and workability while also filling voids within the mixture.

Their incorporation increases concrete strength due to the production of C-S-H with improved properties, as this compound results from the reaction with portlandite. Additionally, they enhance workability, as their high specific surface area demands a greater amount of water. Furthermore, their structure is more compact, as the pores are filled by the small particles, thereby preventing chemical attacks and material corrosion [29].

Methods of obtaining Silica

One of the first methods for obtaining nano-silica was proposed by Beck in 1992, known as the sol-gel process. This method primarily involves forming a colloidal suspension, which subsequently undergoes gelation. During this process, hydrolysis and condensation of salts occur with the addition of catalysts, while acids or bases are introduced at different stages.

The gas-phase method involves reducing quartz in a furnace at temperatures ranging from 1500 to 2000°C. This process produces spherical nano-silica, commonly obtained from the metal industry. Alternatively, nano-silica can be extracted from silicon tetrachloride using hydrogen or oxygen at high temperatures.

The precipitation method utilizes sodium silicate or rice husk. The ashes are heated and washed to remove acids, then further washed to reach a pH of 3. Subsequently, bases are added, and the ashes are washed again until a pH of 7 is achieved, resulting in the extraction of silica [30].

The optimization of synthesis methodologies, such as controlling the pH and sequential acid-base reflux processes, is essential to maximize yield and nanoparticle quality. Similar optimization strategies have been effectively applied in advanced material surface treatments using NSGA-II algorithms [31].

Ilustración 1

Process for nanosilica synthesis.



2. MATERIALS AND METHODS

This study has characterized various resources intended for construction, based on national standards such as the NTE INEN and international standards like ASTM. The materials characterized include sand as fine aggregate, cement, and nano silica.

The process and dosing used for the analysis are presented, along with an in-depth interpretation of the results obtained from the tests conducted on mortar in both its fresh and hardened states. Among the tests performed are flowability, compressive strength at 24 hours, 3 days, 7 days, and 28 days.

The materials used for the characterization and analysis of the mortar behavior in construction are shown in Table 1 below.

Tabla 1

Materials Used

| Material | Source/Specification |
|----------------------|----------------------|
| Fine Aggregate | Copeta Quarry |
| Cement | Master Atenas |
| Water | EPMAPS |
| Oat-based Nanosilica | Self-synthesis |

2.1. NANOSILICA SYNTHESIS.

Separation of the husk and grain.

The methodology consisted of placing the grains in a blender, where the blades, applying mechanical force, separated the husk from the grain. Once this was done, a sieve and vertical movements were used to achieve the complete separation of both elements.

Sample weighing.

The initial weight of the oat husk is recorded in order to determine the yield of the ashes obtained after combustion, expressed as a percentage.

Sample Pyrolysis

The ground oat husks are placed in a heat-resistant container, such as a crucible, to undergo the heating process. A heating mesh is placed between the heat source and the crucible. This step is crucial to ensure the safety of the process and to guarantee an even heat distribution. To ensure the integrity of the container and prevent possible fractures due to direct exposure to the flame, a heating mesh is placed between the heat source and the crucible. This step is critical to maintain process safety and ensure uniform heat distribution.

Ash formation

The crucible with the ashes is placed in a muffle furnace, where the material undergoes a calcination process at a temperature of 1000 °C for a period of 4 hours. This thermal treatment allows the complete conversion of the carbonaceous residue into ashes.

Assembly of the reflux equipment.

First, the universal stand is fixed to the workbench, and the clamps are placed to secure the flask and condenser. Then, a round-bottom flask with an oil bath is mounted, securing the flask to the stand with a clamp. Next, the reflux condenser is connected to the neck of the flask using an adapter or ground joint, securing the connection with another clamp. Afterward, the water hoses are connected to the condenser: one for the inlet (lower part) and one for the outlet (upper part), ensuring proper water flow. The outlet hose is directed to a drain or container. The heating mantle is placed to facilitate the handling of reagents, and finally, the oil is evenly distributed in a pot to ensure proper heating of the flask.

Ash reflux with mineral acids

The ashes are placed in a round-bottom flask, filling at least half of its capacity, and are heated evenly using a pot with oil. The water flow in the condenser is turned on to prevent vapor loss during heating. For the hydrochloric acid treatment, 200 ml of acid are mixed with 100 g of ashes and subjected to reflux at 120 °C for 4 hours. Afterward, the excess acid is evaporated until dryness is achieved. In the nitric acid treatment, the dry ashes are mixed with nitric acid in the same proportion and refluxed again for 4 hours. The excess acid is then evaporated, leaving the ashes ready for the next step in the synthesis.

Washing of ash from acid reflux with distilled water.

After the reflux treatment, the ashes are filtered under vacuum. To completely remove the solid from the reactor, portions of distilled water are added, which are also filtered. The solid is then repeatedly washed with distilled water until the pH of the washing water is between 6 and 7, ensuring the neutralization of the acidic residues. At this point, the ashes contain a higher proportion of silicon dioxide.

Reflux with 3M concentration sodium hydroxide.

The washed ashes, rich in silicon dioxide, are mixed with a 3M NaOH solution (200 ml per 100 g of ashes) and subjected to reflux for 3 hours to ensure a complete reaction. The mixture is then cooled and filtered under vacuum,

separating the solids. The filtrate, which contains sodium silicate, is collected for storage or further processing.

Precipitation and formation of the nanosilica sol-gel system.

The sodium silicate filtrate is neutralized with sulfuric or hydrochloric acid until a pH of 7 is reached, generating a nano-silica gel. The gel is then dried in an oven at 100°C until a dry solid is obtained. Subsequently, it is washed with distilled water until the conductivity is between 17 and 40 $\mu\text{S}/\text{cm}$, removing impurities. Finally, the gel is dried in the oven, resulting in pure nano-silica powder ready for use.

2.2. NANOSILICA

For the use of these particles, the synthesis of nano-silica from oat husk was carried out using the sol-gel method. To obtain the required amount, 4 months were spent, resulting in 150 grams of nano-silica with good purity according to the characterization tests performed. The decision to conduct our own synthesis was due to the availability of the necessary resources and to obtain real properties along with their applications using products found in our country, Ecuador. The oat husk was obtained from San Gabriel, the capital of the Montúfar canton, in the Carchi province.

Validation of silica nanoparticles through laboratory tests.

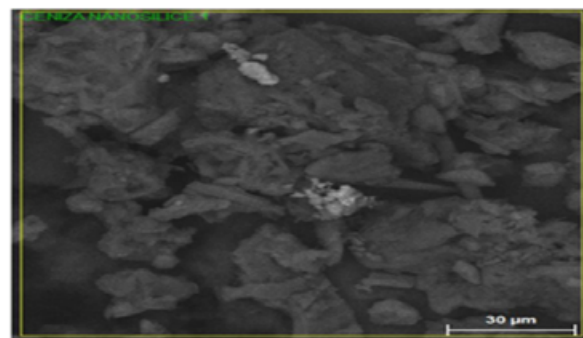
To verify that the purity, quality, and properties of the nano-silica are adequate, Energy Dispersive Spectroscopy (EDS), Scanning Electron Microscopy (SEM), Transmission Electron Microscopy (TEM), and X-Ray Diffraction (XRD) tests were conducted. These tests will allow us to understand the internal structure, composition, and both physical and chemical properties.

Energy Dispersive Spectroscopy (EDS) Assay

This test allows us to perform a microanalysis and quantification of the elements present in the sample, enabling the mapping of different regions represented by different color scales.

Ilustración 2:

Identification and quantification of chemical elements.



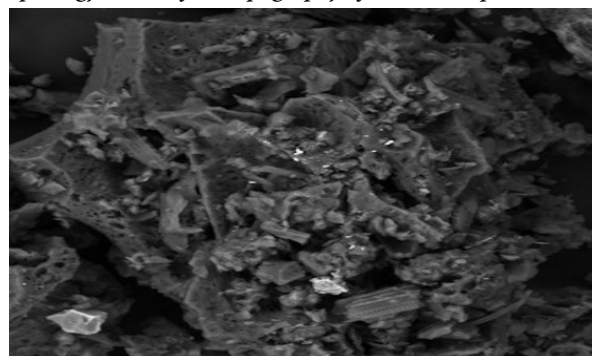
It works by measuring the energy and intensity of the X-rays when the sample is exposed to the electrons from an electron microscope, which interact with the atoms of the sample. The X-rays emitted by the microscope are specific to each element, allowing the images to be recognized by colors [32].

Barrido Microscopy (SEM)

This test allows us to analyze the crystalline structures present in the samples, as well as the topography on the surface, how they interact electrically, and their chemical composition approximately 1 μm from the top of the sample, reaching an analytical magnification of 1,000,000 times, enabling nanometric visualization [33].

Ilustración 3:

Morphology and surface topography of silica nanoparticles.



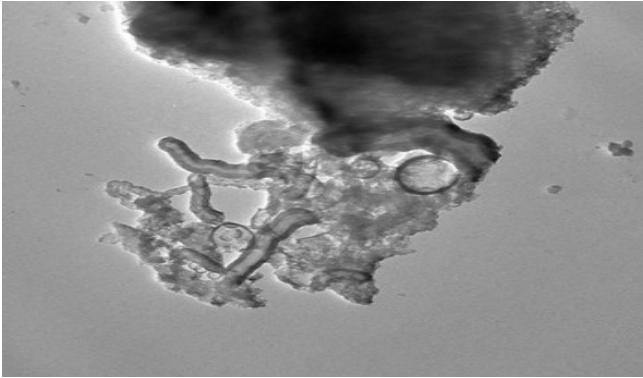
Transmission Electron Microscopy (TEM).

The analysis of TEM images of nano-silica particles allows us to gain a deep understanding of the morphology and structure of the nanoparticles.

The transmission electron microscope operates on the same principle as the optical microscope, except that it uses an electron beam to focus on the specimen and produce the image. It has a wavelength of approximately 0.005 nm, which is equivalent to 100,000 times shorter than the wavelength produced by light [34].

Ilustración 4

Morphology and structure of silica nanoparticles.

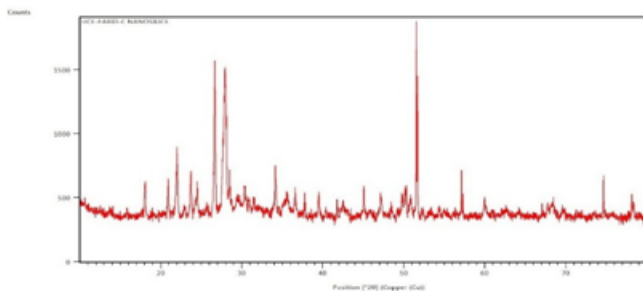


X-Ray Diffraction

The principle of this method is to irradiate a sample with a monochromatic X-ray beam so that the electrons around the atoms vibrate under the action of the X-rays, periodically altering the electric field, causing each electron to act as a secondary wave source that emits electromagnetic waves [35].

Ilustración 5

Spectrogram resulting from X-ray diffraction.



2.3. DESIGN METHODOLOGY.

Material Characterization

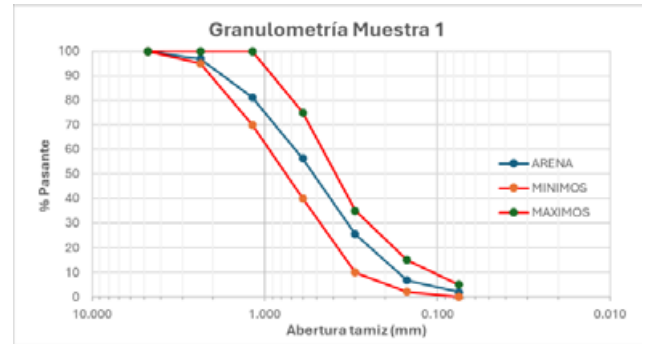
Initially, the characterization of the materials used in the production of mortar cubes is carried out to establish the mix proportions.

Granulometry

The suitability of the fine aggregate size for the mortar is evaluated following the procedure outlined in NTE INEN 696, determining the maximum aggregate size and the fineness modulus. Sieving is performed using the sieves specified by the standard, and the data on the mesh openings of each sieve are plotted alongside the percentage of material passing through each one, comparing them with the limits set by NTE INEN 2536. Three samples of sand are prepared, and granulometric tests are conducted to verify the consistency of the obtained results.

Gráfica 1

Granulometric Distribution



Material Finer than Sieve No. 200

A washing procedure is performed through Sieve No. 200 (75 μ m) using a selected sample of fine aggregate, and the loss of material is determined as a percentage relative to the initial sample, following the procedure outlined in NTE INEN 697.

Tabla 2

Percentage of Finer Material

| MUESTRA | Masa seca Inicial (g) | Masa seca Final (g) | Masa que pasa tamiz 200 | % Material más fino de 75 μ m |
|---------|-----------------------|---------------------|-------------------------|-----------------------------------|
| 1 | 504.60 | 492.00 | 12.60 | 2.5% |
| 2 | 503.50 | 491.40 | 12.10 | 2.4% |
| 3 | 503.70 | 490.10 | 13.60 | 2.7% |

Colorimetry

The content of organic impurities in the fine aggregate is determined by immersing a sand sample in sodium hydroxide for one day. After this period, the color of the resulting liquid is compared with a standardized color palette, following the procedure outlined in NTE INEN 855. This test helps assess the presence of organic materials that could negatively affect the setting and bonding properties of the mortar.

Fotografía 1:

Color Comparison for the Colorimetry Test

Procedimiento: Con el comparador de color normalizado



Numero de orden en el compactador: 1
Resultado: No contiene impurezas inorgánicas

Crumbly Particles

NTE INEN 698 defines the method for determining the percentage of crumbly particles or clay lumps in the fine aggregate. To perform this test, the sample is immersed in distilled water for 24 hours, after which each particle is manually tested by attempting to break it apart with the fingers. The percentage of crumbly particles is then calculated by weighing the particles that break apart and comparing this mass to the total initial mass of the sample. This test helps assess the quality of the fine aggregate, as the presence of crumbly particles can negatively affect the strength and durability of the mortar.

Tabla 3

Presence of Crumbly Particles

| MUESTRA | Masa Inicial (g) | Masa Retenida (g) | % Partículas desmenuzables |
|---------|------------------|-------------------|----------------------------|
| 1 | 25.10 | 24.90 | 0.8% |
| 2 | 25.70 | 25.50 | 0.8% |
| 3 | 25.40 | 25.20 | 0.8% |

Lightweight Particles

The percentage of lightweight particles is determined by immersing a sample of aggregate in a high-density liquid, allowing the lighter particles to remain suspended. The mass of these suspended particles is then measured according to the procedure outlined in NTE INEN 699. This test helps identify any lightweight materials within the aggregate, which can affect the strength and performance of the mortar.

Tabla 4

Presence of Lightweight Particles.

| MUESTRA | Masa Seca (g) | Masa Seca partículas flotantes (g) | % Partículas livianas |
|---------|---------------|------------------------------------|-----------------------|
| 1 | 216.02 | 0.55 | 0.3% |
| 2 | 197.22 | 0.75 | 0.4% |
| 2 | 229.70 | 0.90 | 0.4% |

Sulfate Degradation

Following the procedure outlined in NTE INEN 863, the specified aggregate samples are subjected to a repetitive process of exposure and drying in a sulfate solution. After completing the test, each sample is weighed to determine the effect caused by the sulfate exposure. This test helps assess the aggregate's durability and resistance to sulfate-induced degradation, which can negatively affect the performance of the mortar.

Tabla 5

Percentage of Loss Due to Sulfate Degradation

| FRACCIÓN | | Masa inicial (g) | Masa final (g) | % de pérdida |
|------------|---------------------|------------------|----------------|--------------|
| Pasa tamiz | se retiene en tamiz | | | |
| 600µm | 300µm | 100.00 | 99.20 | 1% |
| 1,18mm | 600µm | 100.00 | 99.00 | 1% |
| 3,36mm | 1,18mm | 100.00 | 98.70 | 1% |

Specific Weight and Absorption Capacity

The specific weight and absorption capacity are determined following the procedure established in NTE INEN 856. This involves bringing the aggregate sample to the Saturation with Surface Dry (SSD) state and measuring its mass. Then, the volume of the sample is determined, and it is dried to measure its mass again. Finally, the required values are calculated using the formulas specified in the standard.

Loose and Compacted Density

Following the procedure outlined in NTE INEN 858, the samples are placed in a standardized container, both in loose and compacted states. The mass and volume of the fine aggregate sample are then determined.

Cement Density

According to NTE INEN 156, a Le Chatelier flask, diesel, and a cement sample are used. By measuring the mass and volume of the cement, its density can be determined. The test is repeated three times to validate the results, which are presented in the following table.

Mix Design

A mortar mix is prepared to produce 9 cubes for the compressive strength test, following the material dosage established in NTE INEN 488. For the mix, type N cement from Atenas is used, for which no exact quantity is specified. An initial water/cement ratio of 0.52 is used and adjusted until the flow required by the NTE INEN 488 standard is achieved.

Material Mixing

The procedure for preparing the mortar mix according to the NTE INEN 155 standard includes: drying the sand for 24 hours, sieving the cement to remove clumps, and controlling the water temperature. 740 g of cement and 2035 g of sand are weighed, and the water volume is measured based on the water/cement ratio. The mixing process consists of several stages: first, adding water and cement at low speed, then incorporating the sand, switching to medium speed to mix, homogenizing the

mixture, and finally mixing again at medium speed to achieve a uniform consistency.

Determination of the Mix Flow

According to NTE INEN 488, the flow of the mortar mix must be 110 ± 5 , measured in accordance with NTE INEN 2502. The procedure includes cleaning and preparing the flow table, filling and compacting the mold with mortar in two stages, smoothing the surface, and allowing it to rest for 1 minute. Then, the mold is removed, the table is dropped 25 times in 15 seconds, and the resulting diameter is measured at four points. Finally, the measurements are summed to calculate the total flow of the mix.

The mortar produced with Type N cement demonstrates adequate workability. However, when nanomaterials are incorporated as a partial cement replacement, a reduction in workability is observed, leading to deficiencies in its fresh-state properties. [36]

Specimen Preparation

The procedure for preparing mortar cubes, according to NTE INEN 488, includes cleaning the molds, applying release agent, and mixing the remaining mortar at medium speed for 15 seconds. Then, the molds are filled, compacted in two stages with uniform strikes, the surface is smoothed with a trowel, the molds are labeled, and they are transferred to the curing chamber under controlled conditions.

Addition of Nanosilica to the Mortar Mix

The influence of nanosilica on the compressive strength of the mortar will be evaluated at 1, 7, and 28 days, incorporating 0.25%, 0.50%, 0.75%, and 1.0% into different mixes. For this, the amount of nanosilica will be calculated based on the weight of the cement, partially replacing it. The dispersion will be prepared by mixing the nanosilica with the water before incorporating all the mortar components. Tests will be repeated for each dosage, and the results will be compared to determine the optimal proportion.

As this is a specialized concrete incorporating materials such as nano-silica, a specific mixing methodology is required to ensure proper adhesion of the nano-silica nanoparticles within the mixture. It is recommended to reserve a minimum amount of water to effectively dissolve the nano-silica, ensuring a homogeneous blend. [37]

Curing and Compressive Strength

The curing conditions for fresh mortar typically involve maintaining a constant temperature of approximately 23°C and a relative humidity of 50% during the initial setting phase. For hardened mortar, the samples are kept at a temperature of $23 \pm 2^\circ\text{C}$ and a relative humidity of at least 50% for periods of 4, 7, 14, and 28 days. [38]

The compressive strength test of mortar cubes according to NTE INEN 488 includes demolding the specimens without damaging them and placing them under controlled humidity and temperature conditions. Before the test, the dimensions of the cubes are measured and recorded in the compression machine. The specimen is placed in the machine, correctly centered, and the load is applied, recording the maximum force and stress in MPa at the moment of failure. The variation in permissible ages according to the standard is also considered.

When incorporated into the matrix of cement-based materials such as concrete, nanosilica has been demonstrated to significantly enhance performance. This study reveals that the addition of nanosilica can increase the strength and durability of concrete by up to four times. Both microsilica and nanosilica exhibit high pozzolanic activity, enabling them to regulate undesirable crystallization within the concrete matrix. [39]

Absorption Capacity

The absorption test in mortars determines the amount of water the material can absorb within a specified time, indicating its porosity. The specimens are cured for 28 days and then completely dried in an oven before recording their initial weight (W_1). Subsequently, they are submerged in water at room temperature for 24 hours, ensuring the absence of trapped air bubbles. Afterward, the specimens are removed and weighed again to obtain the final weight (W_2). The absorption is calculated using the equation: $\text{Absorption (\%)} = ((W_2 - W_1) / W_1) \times 100$, where W_1 is the dry weight and W_2 is the weight after immersion.

Permeability

To determine the permeability of the mortar, the contact angle test, also known as the drop test, will be used. This test allows us to measure the ability of a liquid to wet a solid surface [40]. It involves placing a drop on the surface and measuring the angle formed between the tangent of the drop and the surface of the material at the contact point. The materials and procedure are as follows.

3. RESULTS AND DISCUSSION

3.1. YIELD.

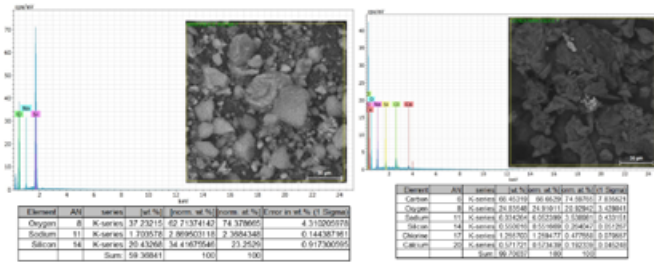
Based on the results obtained from nano-silica, it is considered that the yield is low; however, the presence of silica in the oat husk is a significant advantage. The advantage lies in the fact that being an

abundant agro-industrial byproduct with very low cost, it makes it an economical and sustainable alternative. This allows for the reuse of these wastes to promote the circular economy and reduce environmental impact.

3.2. ENERGY DISPERSIVE SPECTROSCOPY (EDS)

Gráfica 2:

On the left is the composition of the nanosilica and on the right the ash residue of synthesis *síntesis*.

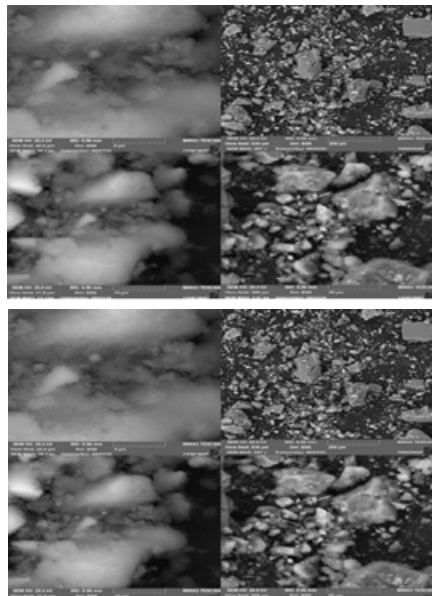


In the graph on the left, we can discuss a high relative purity, despite the presence of sodium residues, as it shows a high content of oxygen and silicon, both in weight and atoms, suggesting that the material is predominantly silica. The graph on the right shows that the silica content in the sample is low, indicating that the synthesis process has not been fully efficient in producing nano-silica. Therefore, these ashes could not be treated as they would not contain a significant amount of silica, considering the time it takes.

3.3. SCANNING ELECTRON MICROSCOPY (SEM)

Image 1

On the left is the SEM image of the nanosilica and on the right the ash residue of the synthesis.

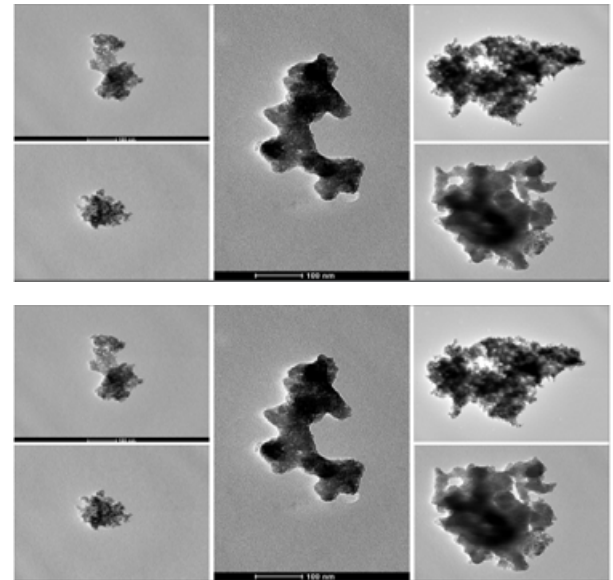


The left side, we can observe that the aggregates are spherical or nearly spherical, which is characteristic of nano-silica synthesized by methods such as sol-gel. Additionally, the agglomeration indicates that the particles are interacting with each other due to electrostatic or van der Waals attraction. On the right side, the particles appear to have very irregular and rough surfaces. This is typical of residues that have been subjected to high temperatures but have not been fully calcined. The roughness may indicate the presence of pores and gaps left as a result of burning the organic material. Some of the observed structures appear to be fibrous or laminar. These could be remnants of the original biomass, such as traces of plant fibers.

3.4. TRANSMISSION ELECTRON MICROSCOPY (TEM)

Image 2

On the left is the TEM image of the nanosilica and on the right the ash residue of the synthesis.

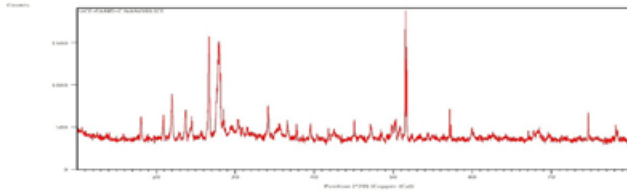


The tests show that for the nano-silica, by performing the following analysis, we can observe that the particle size obtained by this methodology is 8.04 nm, which is close to the range typically considered for nano-silica particles, which usually fall between 1 and 100 nm. On the other hand, for the ashes, the particle size obtained by this methodology is 143.816 nm, which is outside the range considered for nano particles.

3.5. X-RAY DIFFRACTION (XRD)

Gráfica 3

Nanosilica diffractogram shown.



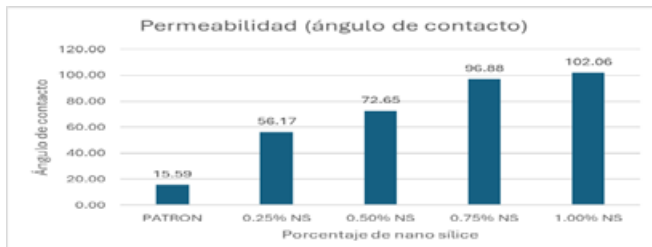
One of the most representative peaks is found at 26.6° , indicating the presence of quartz (crystalline SiO_2), as this position is characteristic of this material. Quartz is one of the most common forms of silicon dioxide, which is consistent with the fact that the sample is nano-silica. The presence of smaller peaks could be related to the presence of other silica phases or impurities in the sample.

The incorporation of nano-silica into cementitious matrices has been shown to significantly enhance mechanical properties by reducing porosity and improving microstructural densification, aligning with recent findings in high-performance mortar development [41].

3.6. PERMEABILITY

Gráfica 4

Contact angle of conventional mortar and with the addition of nanosilica.

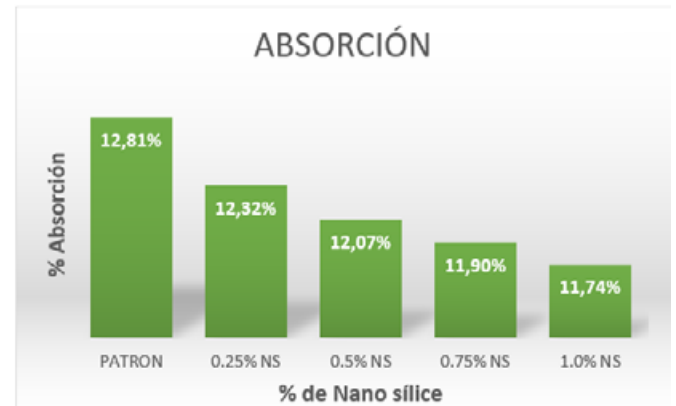


The contact angle values obtained from the conventional mortar samples and mortar with the addition of nano-silica at 28 days of curing are presented. These values are key to evaluate the wettability of the surface, which is correlated with the permeability of the material. The angle increases with the increase in the nano-silica content, ranging from the lowest value of 15.59° for the control mixture, indicating a high affinity of water with the surface, to the maximum value of 102.06° with the addition of 1.00% nano-silica, showing a hydrophobic trend.

3.7. ABSORPTION

Gráfica 5

Absorption percentage depending on the nanosilica percentage.

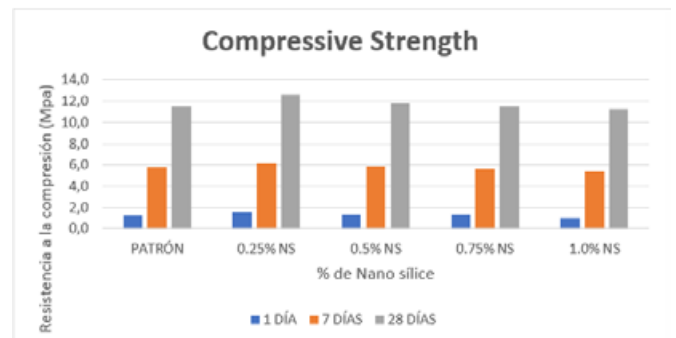


The graph shows the relationship between the absorption percentage and the nanosilica content (% NS). It is observed that as the concentration of nanosilica increases, the absorption percentage progressively decreases. The highest absorption value (12.81%) is found in the reference sample (PATRÓN), while the lowest value (11.74%) corresponds to the sample with 1.0% nanosilica. This indicates that the incorporation of nanosilica reduces the absorption of the material.

3.8. COMPRESSIVE STRENGTH

Gráfica 6:

Compressive strength with different nanosilica percentages at different ages.

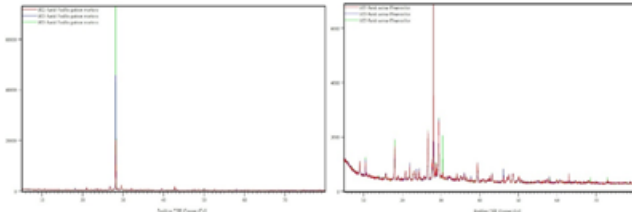


The graph shows the evolution of compressive strength (in MPa) as a function of nanosilica content and curing time (1, 7, and 28 days). The samples with 0.25% and 0.5% nanosilica show a slight improvement in strength compared to the reference, especially at 28 days. However, at higher concentrations (0.75% and 1.0% NS), the strength tends to stabilize or even slightly decrease. This suggests that there is an optimal point in the addition of nanosilica to improve compressive strength without compromising the material's structure.

3.9. X-RAY DIFFRACTION (XRD) MORTAR CUBES.

Gráfica 7

The diffractogram is shown on the left of the conventional mortar and on the right with the addition of 0.25% nanosilica.



In the control sample, the high peak near 30° suggests the predominance of residual alite or belite, indicating incomplete hydration (less than 100%). Additionally, the small peaks between 18° and 34° suggest typical hydration without substantial chemical modifications. On the other hand, with the addition of nano-silica, a reduction in the relative intensity of the portlandite peak, typically located around 18° , 34° , and 47° in 2θ , is observed. This reduction implies that nano-silica has reacted with portlandite to form more C-S-H gel (calcium silicate hydrate), which results in a denser cement matrix, thereby improving mechanical properties. The reduction of free portlandite means there is less material available to react with CO_2 or sulfates, thus enhancing the material's durability in aggressive environments. This occurs because the reaction of nano-silica generates products that fill the capillary pores, reducing total porosity and improving mechanical strength, which in turn leads to long-term durability.

3.10. ANALYSIS OF THE COST OF PRODUCTION OF NANOSILICA.

According to the calculation, it is observed that producing 100 grams of nano-silica costs \$368.97. When compared to the commercial prices of Aerosil 200, which is around \$161.95 for 4.5 kg in the United States, the laboratory production cost is significantly higher than the market value. This indicates that at an industrial level, the methods are more efficient and cost-effective.

4. CONCLUSIÓN

- The synthesis of nano-silica from oat husks using the sol-gel method proved to be a viable process, achieving a yield of 2.79%, showing a significantly higher efficiency compared to the study conducted by the pharmaceutical laboratory of the Faculty of Chemical Sciences at the Central University of Ecuador, which achieved a yield of 0.98% using the extraction and gravimetry method. This difference suggests that the sol-gel method optimizes the recovery of silica from agro-industrial waste, thus improving its viability

for applications in cementitious materials. Furthermore, the ability to adjust synthesis parameters to control particle morphology and size opens new opportunities for its incorporation into high-performance materials.

- The characterization analysis conducted through the EDS, SEM, TEM, and XRD tests allowed the evaluation of both the chemical composition and morphology of the nano-silica and oat husk ash. The EDS spectra confirmed the high purity of the synthesized nano-silica, with an approximate concentration of SiO_2 (90%), while the remaining content consisted of trace impurities. In contrast, the oat husk ashes showed approximately 1% silica. Regarding the images obtained by SEM and TEM, it was revealed that the synthesized nano-silica exhibited spherical particles with an approximate size of 8-15 nm and a homogeneous distribution. On the other hand, the oat husk ashes presented larger aggregates with dimensions greater than 100 nm. This finding suggests that controlling the synthesis process plays a crucial role in obtaining nanoparticles with optimized properties. The X-ray test of the nano-silica revealed the presence of amorphous phases characteristic of SiO_2 , with a broad peak at $2\theta = 22^\circ$, which is favorable for its reactivity in cementitious applications. This suggests that the sol-gel synthesis method enables the production of a material with high potential reactivity in cement matrices.
- The study on the influence of nanosilica addition in mortars reveals that compressive strength varies depending on the addition percentage and curing time, showing better results at lower doses. At 1 and 7 days, the mix with 0.25% nanosilica exhibited the highest strength compared to mixes with 0.5%, 0.75%, and 1%, while higher doses did not provide consistent improvements. At 28 days, the trend remains, with 0.25% reaching the highest strength (12.6 MPa). This suggests that small amounts of nanosilica optimize strength, but higher doses may not be beneficial.
- This study evaluated the economic feasibility of producing nano-silica from oat husks, with an approximate cost of \$368.97 per 100 grams of product under laboratory conditions, using agro-industrial waste, promoting the circular economy and environmental sustainability. By utilizing an abundant, low-cost waste material and the ability to customize the properties of the material according to its specific application, its production in laboratories could be justified due to particular technical requirements. Under current conditions, however, the production is not competitive.

REFERENCES

- [1] R. Salamanca, "La Tecnología de los Morteros," Diciembre 2001. [En línea]. Disponible en: <https://www.redalyc.org/pdf/911/91101107.pdf>. [Último acceso: 6 Agosto 2024].
- [2] INEN, "Morteros para unidades de mampostería," Enero 2010. [En línea]. Disponible en: <https://drive.google.com/file/d/1iazTpPDp6H0oNMoryoeKryG4FaNm-gHrI/view>. [Último acceso: 7 Agosto 2024].
- [3] M. Alvansazyazdi, N. Salgado, A. Borghei, S. Camino y M. Guzmán, "Web-Based Executive Dashboard Reports for Public Works Clients in Construction Industry," en *[Nombre de la Conferencia o Libro si se conoce]* pp. 285-294, 2019.
- [4] A. Global, "Nanotecnología en la construcción," 6 Noviembre 2023. [En línea]. Disponible en: <https://www.arcus-global.com/wp/nanotecnologia-en-la-construccion/>. [Último acceso: 7 Agosto 2024].
- [5] BricKaffix, "Nanotecnología en la construcción, Innovación y Eficiencia," 25 Mayo 2023. [En línea]. Disponible en: <https://brickaffix.mx/nanotecnologia-construccion/>. [Último acceso: 7 Agosto 2024].
- [6] M. Alvansazyazdi, H. Alvansaz, M. Hakakian, N. Salgado y A. Camino Solórzano, "An Investigation and Presentation of a Model for Factors Influencing the Agility of Human Resources: A Case Study of Yazd Electricity Distribution Company," In Á. Rocha *et al.* (Eds.), pp. 823-834, 2019.
- [7] N. Salgado, J. Guña, C. Escobar y M. Alvansazyazdi, "Result of the Methodology for Learning English Distance with the Use of TICs. Case Study: Central University of Ecuador," In Á. Rocha *et al.* (Eds.), WorldCIST', n° 19, pp. 227-233, 2019.
- [8] L. Moragues y M. Sanchez, "Influencia de la adición de nano sílice en algunos aspectos de la durabilidad, en hormigones autocompactantes de alta resistencia," 2013. [En línea]. Disponible en: https://oa.upm.es/29970/1/INVE_MEM_2013_165946.pdf. [Último acceso: 7 Agosto 2024].
- [9] Instituto Ecuatoriano de Normalización (INEN), *Morteros para unidades de Mampostería*. Quito, Ecuador, 2010
- [10] M. Khorami, M. Khorami, H. Motahar, M. Alvansazyazdi, M. Shariati, A. Jalali y M. Tahir, "Evaluation of the seismic performance of special moment frames using incremental nonlinear dynamic analysis," *Structural Engineering and Mechanics*, vol. 63, n° 2, pp. 259-268, 2017.
- [11] M. Alvansazyazdi, A. Villalba, S. Saltos, J. Santamaria, A. Cadena, M. Leon, L. Leon, P. Bonilla, B. Heredia, J. Bucheli, A. Debut, y M. Feizbahrh, "Enhancing Sustainable Construction: An Evaluation of NanoGraphene's Effectiveness in Mortar Composition," *Int. J. Eng. Technol. Sci.*, 2023.
- [12] M. Şişman, E. Teomete, J. Yanik, y U. Malayoglu, "The effect of nano-biochar produced from various raw materials on flow and mechanical properties of mortar," *Constr. Build. Mater.*, 2025.
- [13] H. Du, S. Du, y X. Liu, "Durability performances of concrete with nano-silica," *Constr. Build. Mater.*, 2014.
- [14] M. M. Badalyan, N. G. Muradyan, R. S. Shainova, y A. A. Arzumanyan, "Effect of Silica Fume Concentration and Water-Cement Ratio on the Compressive Strength of Cement-Based Mortars," *Constr. Build. Mater.*, 2024.
- [15] M. Usman *et al.*, "Study on Relationship Between Mechanical Properties and Water Absorption Characteristics of Mortars by Using Digital Image Correlation Method (DICM)," *Materials*, 2025.
- [16] C. M. Stolz, A. Rysdyk, M. Amario, M. Najjar, E. G. Vazquez, y A. N. Haddad, "Evaluation of Water Vapor Permeability in Mortars Produced with Crystallizing Additive," *NanoWorld J.*, 2023.
- [17] A. Rityparna y S. Mozumdar, "Nanotecnología," *SpringerNATURE*, pp. 35-36, 12 Mayo 2013.
- [18] G. Williams, C. Haynes, M. Tarifas, C. Caltagirone, J. Rugallo y F. Vendaval, "Advances in applied supramolecular technologies," *Chemical Society Reviews*, vol. 50, pp. 2737-2763, 22 Septiembre 2021.
- [19] R. Checkers, P. MarshallJosh, P. DvorakLiam, K. B. TwightLan ChenKentaro, E. AndreevaAlexandra, E. F. OverlandThomas, K. CozzolinoCarl y Brozek, "Size-Dependent Properties of Solution-Processable Conductive MOF Nanocrystals," *J. Am. Chem. Soc.*, pp. 5784-5794, 30 Enero 2022.
- [20] M. Alvansazyazdi y J. Rosero, "The pathway of concrete improvement via nano-technology," *INGENIO*, vol. 2, n° 1, p. 1, 2019.
- [21] S. Sim y N. Wong, "Nanotechnology and its use in imaging and drug delivery," 5 Marzo 2021. [En línea]. Disponible en: <https://www.spandidos-publications.com/10.3892/br.2021.1418>. [Último acceso: 24 Septiembre 2024].
- [22] A. Barhoum, M. García, J. Jeevanandam y E. Hussien, "Review on Natural, Incidental, Bioinspired, and Engineered Nanomaterials: History, Definitions, Classifications, Synthesis, Properties, Market, Toxicities, Risks, and Regulations," 6 Enero 2022. [En línea]. Disponible en: <https://www.mdpi.com/2079-4991/12/2/177>. [Último acceso: 24 Septiembre 2024].

- [23] A. Sosa, G. Romanelli y L. Pizzio, "Nanoestructuras de sílice, con diámetro y distribución de mesoporos variable, modificadas con ácido tungstosfórico como catalizadores en la síntesis de quinoxalinas," 18 Abril 2020. [En línea]. Disponible en: <https://www.redalyc.org/journal/3090/309063462006/html/>. [Último acceso: 7 Agosto 2024].
- [24] J. Manazo, M. Lozano, y M. Vallet-Regí, "Nanopartículas mesoporosas de sílice y la osteoporosis," Diciembre 2022. [En línea]. Disponible en: https://scielo.isciii.es/scielo.php?script=sci_arttext&pid=S1889-836X2022000400001 [Accedido el 25 de Septiembre de 2024].
- [25] M. Alvansazyasdi, C. Bombon y B. Rosero, "Estudio de la incorporación de nanosílice en concreto de alto desempeño (hpc)," *INGENIO*, vol. 5, n° 1, pp. 12-21, 2022.
- [26] M. Alvansaz, B. Arévalo y A. Julio, "Adoquines de hormigón ecoamigables fabricados con la incorporación de una Mezcla de Micro-Nano Sílice" *INGENIO*, vol. 5, n° 1, pp. 34-42, 2022.
- [27] L. W. Morales, M. Alvansazyazdi, *et al.*, "Prevención de la contaminación por la fabricación de hormigones con nanopartículas," ResearchGate, 2020.
- [28] M. AlvansazYazdi, R. Zakaria, M. Mustaffar, M. Majid, R. MohamadZin, M. Ismail y K. Yahya, "Bio-composite materials potential in enhancing sustainable construction," *Desalination and Water Treatment*, vol. 52, pp. 3631-3636, 2014.
- [29] P. Damodaran, M. Nagarajan, and L. Thangasamy, "Assessing the Durability, Mechanical, and Microstructural Properties of Nanosilica-enhanced Coconut Shell Concrete: A Sustainable Approach," *J. Environ. Nanotechnol.*, 2024.
- [30] A. Moreno, "Optimización en la incorporación de nanoadiciones al cemento para la mejora de sus prestaciones y durabilidad," 2018. [En línea]. Disponible en: <https://1library.co/document/zw5073lz-optimizacion-incorporacion-nanoadiciones-cemento-mejora-prestaciones-durabilidad.html>. [Último acceso: 8 Agosto 2024].
- [31] A. Golsha, M. Rezazadeh Shirdar, S. Gohery y M. Alvansazyazdi, "Optimization of Pre-Treatment Parameters before Diamond Coating using Non-Dominated Sorting Genetic Algorithm (NSGA-II)," *Advanced Materials Research*, n° 463-464, 399-405, 2012.
- [32] BRUKER, "What is EDS/EDX? introducing Energy Dispersive X-Ray Spectroscopy," 2024. [En línea]. Disponible en: <https://www.bruker.com/en/landingpages/bna/technology/what-is-eds.html>. [Último acceso: 15 Septiembre 2024].
- [33] A. Erol, "High-Magnification SEM Micrograph of siloxanes," 17 Diciembre 2018. [En línea]. Disponible en: <https://www.intechopen.com/chapters/64959>. [Último acceso: 15 Septiembre 2024].
- [34] F. Morkobi, "Transmission Electron Microscope (TEM)," 19 Mayo 2022. [En línea]. Disponible en: <https://microbenotes.com/transmission-electron-microscope-tem/>. [Último acceso: 15 Septiembre 2024].
- [35] DRAWELL, "The ultimate guide to XRD-From theory to practice," 18 Noviembre 2022. [En línea]. Disponible en: <https://www.drawellanalytical.com/the-ultimate-guide-to-xrd-from-theory-to-practice/>. [Último acceso: 15 Septiembre 2024].
- [36] M. Alvansazyazdi, J. Fraga, E. Torres, G. Bravo, J. Santamaria, M. Leon, A. Cadena, L. Leon, P. Bonilla, B. Heredia, A. Debut, M. Feizbahr, y R. Yuri, "Comparative Analysis of a mortar for plastering with hydraulic cement type HS incorporating nano-iron vs cement-based mortar for masonry type N," *Int. J. Eng. Technol. Sci.*, 2024.
- [37] M. Alvansazyazdi, D. Farinango, J. Yaucan, A. Cadena, J. Santamaria, P. M. Bonilla-Valladares, M. Leon, A. Debut, M. Feizbahr, L. Leon, y B. Ayala, "Exploring Crack Reduction in High-Performance Concrete: The Impact of Nano-Silica, Polypropylene, and 4D Metallic Fibers," *Int. J. Eng. Technol. Sci.*, 2023.
- [38] M. Alvansazyazdi, J. Figueroa, A. Paucar, G. Robles, M. Khorami, P. M. Bonilla-Valladares, A. Debut, y M. Feizbahr, "Nano-silica in Holcim general use cement mortars: A comparative study with traditional and prefabricated mortars," *Adv. Concr. Constr.*, 2024.
- [39] M. Alvansazyazdi, J. Tapia, y A. Barrionuevo, "Study of an Environmentally Friendly High-Performance Concrete (HPC) Manufactured with the Incorporation of a Blend of Micro-Nano Silica," *Rev. Científica Arq. Urbanismo*, 2024.
- [40] M. Alvansazyazdi, F. Alvarez, J. Pinto, M. Khorami, P. Bonilla, A. Debut, y M. Feizbahr, "Evaluating the Influence of Hydrophobic Nano-Silica on," *Sustainability*, pp. 3-4, 2023.
- [41] M. Alvansazyazdi, J. Figueroa, A. Paucar, G. Robles, M. Khorami, P. M. Bonilla-Valladares, A. Debut y M. Feizbahr, "Nano-silica in Holcim General Use Cement Mortars: A Comparative Study with Traditional and Prefabricated Mortars," *Advances in Concrete Construction*, vol. 17, n° 3, pp. 135-150, 2024.
- [42] J. Gonzalez, "ESTUDIO DEL MORTERO DE PEGA USADO EN EL CANTÓN CUENCA PROPUESTA DE MEJORA UTILIZANDO ADICIONES DE CAL," 2016. [En línea]. Disponible en: <https://dspace.ucuenca.edu.ec/bitstream/123456789/23664/1/TESIS%20final%20.pdf>. [Último acceso: 7 Agosto 2024].
- [43] A. Romero, "DISEÑO EXPERIMENTAL DE UN MORTERO DE CEMENTO REFORZADO CON FIBRAS NATURALES DE ORIGEN ANIMAL "PLUMAS DE AVES"" 2022. [En línea]. Disponible en: <https://www.studocu.com/ec/document/universidad-lai-ca-vicente-rocafuerte-de-guayaquil/arquitectura/t-uide-0328-material/46344469..> [Último acceso: 7 Agosto 2024].

- [44] S. Correa, "Dosificación morteros," de *Dosificación morteros*, 1985, pp. 17-23.
- [45] F. Gottschalk, B. Debray, F. Klaessing y P. Barry, "Predicting accidental release of engineered nanomaterials to the environment," 2 Febrero 2023. [En línea]. Disponible en: <https://www.nature.com/articles/s41565-022-01290-2>. [Último acceso: 24 Septiembre 2024].
- [46] D. Heras, "Morteros de cemento con nano-adiciones de hierro y sílice,"
- [47] R. Chudley y R. Greeno, "Building Construction Handbook," 2008. [En línea]. Disponible en: http://students.aiu.edu/submissions/profiles/resources/onlineBook/s6C5h7_construction-handbook-chudley.pdf.
- [48] G. Rivera, *Concreto Simple*. Cauca, Colombia, 2009.
- [49] V. Cervantes, "Aplicaciones Generales de la nanotecnología en el campo de la Construcción," *PITRA*, 2011.
- [50] L. Molina y M. Garzón, "Propiedades de concretos y morteros modificados con nanomateriales: Estado del Arte," *Arquetipo*, vol. 14, pp. 81-98, 2017.
- [51] Graphenemex, "Nanotecnología y protección contra la corrosión: La era del Óxido de grafeno," 2018. [En línea]. Disponible en: <https://www.graphenemex.com/tag/es-malte-alquidamico/>.
- [52] D. Sanchez de Guzman, *Tecnología del concreto y del mortero*. Santafé de Bogotá: Bahandar Editores Ltda, 2001.
- [53] A. Cardona, "la versatilidad del mortero, su importancia y sus posibilidades en la construcción," universidad militar nueva granada, Bogotá, 2021.
- [54] BRUKER, "What is EDS/EDX? Introducing Energy Dispersive X-Ray Spectroscopy," 2024. [En línea]. Disponible en: <https://www.bruker.com/en/landingpages/bna/technology/what-is-eds.html>. [Último acceso: 15 Septiembre 2024].
- [55] A. Erol, "High-Magnification SEM Micrograph of Siloxanes," 17 Diciembre 2018. [En línea]. Disponible en: <https://www.intechopen.com/chapters/64959>. [Último acceso: 15 Septiembre 2024].
- [56] F. Mokobi, "Transmission Electron Microscope (TEM)-Definition, Principle, Images," 19 Mayo 2022. [En línea]. Disponible en: <https://microbenotes.com/transmission-electron-microscope-tem/>. [Último acceso: 15 Septiembre 2024].
- [57] S. K. S. S. M. Ranjana*, "NANOSILICA'S INFLUENCE ON CONCRETE HYDRATION, MICROSTRUCTURE, AND DURABILITY," *JOURNAL OF APPLIED ENGINEERING SCIENCES*, 2024.
- [58] T. Ji, "Preliminary study on the water permeability and microstructure of concrete incorporating nano-SiO₂," *Cement and Concrete Research*, 2015.
- [59] R. Salamanca Correa, "Dosificación de morteros," vol. 3, n° 2, pp. 17-23, 1985.
- [60] X. Chen, E. Gruyaert, Ö. Cizer y J. Li, "Materconstrucc," 2023. [En línea]. Disponible en: <https://materconstrucc.revistas.csic.es/index.php/materconstrucc/article/download/3501/4271?inline=1>.
- [61] G. O. S. R. Caiza C, "Permeabilidad de diferentes dosificaciones de mortero utilizados en la industria de la construcción en el Ecuador," *UNIVERSIDAD CENTRAL DEL ECUADOR*, 2020.
- [62] M. Alvansazyazdi, F. Alvarez-Rea, J. Pinto-Montoya, M. Khorami, P. M. Bonilla-Valladares, A. Debut, y M. Feizbahr, "Evaluating the Influence of Hydrophobic Nano-Silica on Cement Mixtures for Corrosion-Resistant Concrete in Green Building and Sustainable Urban Development," *Sustainability*, 2023.

ANNEXES

Table 6

Percentage of Absorption of Fine Aggregate.

| MUESTRA 1 | |
|--|--------|
| Masa picnómetro vacío (g): | 188.7 |
| Masa picnómetro + Arena SSS (g): | 684.2 |
| Masa picnómetro + agua + Arena S | 996.1 |
| Masa del picnómetro con agua (g): | 686.23 |
| Densidad del agua (g/cm ³): | 1.0 |
| Masa de agua desalojada (g): | 309.9 |
| Masa de la muestra SSS (g): | 495.5 |
| Volumen de agua desalojado (cm ³): | 185.67 |
| Masa de la muestra SSS (g): | 490.25 |
| Masa de la muestra seca (g): | 483.2 |
| RESULTADOS: | |
| Peso específico (g/cm ³): | 2.7 |
| Peso específico (kg/m ³): | 2670 |
| Absorción % | 1.5 |

Table 7

Loose and Compacted Density of Sand.

| Densidad Suelta Arena | | | |
|------------------------------|--------|--------|--------|
| Masa molde (g): | 628.9 | | |
| Volumen molde (cm3): | 1000 | | |
| MUESTRA | 1 | 2 | 3 |
| Masa del arido+ molde 1 (g): | 2244.2 | 2257.1 | 2243.2 |
| Masa del arido+ molde 2 (g): | 2245.3 | 2262.5 | 2245.7 |
| Masa del arido+ molde 3 (g): | 2245.1 | 2259.4 | 2247.7 |
| Promedio (g): | 2244.9 | 2259.7 | 2245.5 |
| Densidad del agua (kg/m3): | 998.0 | | |
| RESULTADOS: | | | |
| Masa unitaria (g/cm3): | 1.62 | 1.63 | 1.62 |
| Masa unitaria (kg/m3): | 1620 | 1630 | 1620 |

| Densidad Suelta Arena | | | |
|------------------------------|--------|--------|--------|
| Masa molde (g): | 628.9 | | |
| Volumen molde (cm 3): | 1000 | | |
| MUESTRA | 1 | 2 | 3 |
| Masa del arido+ molde 1 (g): | 2244.2 | 2257.1 | 2243.2 |
| Masa del arido+ molde 2 (g): | 2245.3 | 2262.5 | 2245.7 |
| Masa del arido+ molde 3 (g): | 2245.1 | 2259.4 | 2247.7 |
| Promedio (g): | 2244.9 | 2259.7 | 2245.5 |
| Densidad del agua (kg/m 3): | 998.0 | | |
| RESULTADOS: | | | |
| Masa unitaria (g/cm 3): | 1.62 | 1.63 | 1.62 |
| Masa unitaria (kg/m 3): | 1620 | 1630 | 1620 |

Table 8

Average Cement Density.

| Densidad del cemento | | | |
|--|--------|--------|--------|
| MUESTRA # | 1 | 2 | 3 |
| Masa cemento inicial: | 64.02 | 64 | 64.02 |
| Lectura Inicial (vol. Gasolina en frasco): | 0.1 | 0.1 | 0.1 |
| Lectura Final (vol. Gasolina en frasco): | 23.6 | 23.4 | 23.4 |
| Volumen desplazado: | 23.5 | 23.3 | 23.3 |
| Peso diesel + muestra: | 390.26 | 390.29 | 390.88 |
| RESULTADOS: | | | |
| Densidad del cemento: | 2.72 | 2.75 | 2.75 |
| Promedio | 2.74 | | |

Table 9

Material Dosage According to NTE INEN 488.

| MATERIAL | NÚMERO DE ESPECÍMENES | |
|---|-----------------------|-------|
| | 6 | 9 |
| Cemento, g | 500 | 740 |
| Arena, g | 1.375 | 2.035 |
| Agua, cm ³ | | |
| - Portland (a/c = 0,485) | 242 | 359 |
| - Portland con incorporador de aire (a/c = 0,460) | 230 | 340 |
| - Otros (para un flujo de 110 ± 5) | ----- | ----- |



Table 10

Results of nanosilica synthesis.

| UNIVERSIDAD CENTRAL DEL ECUADOR FACULTAD DE INGENIERÍA Y CIENCIAS APLICADAS CARRERA DE INGENIERÍA CIVIL | |
|---|---|
| Realizado por: | Carlosama A. & Rosillo J. |
| Proyecto: | Síntesis de nano sílice a partir de la cáscara de avena para modificar las propiedades físicas y mecánicas del mortero con un enfoque eco amigable. |
| RENDIMIENTO DE LA SINTESIS DE NANOSÍLICE | |
| PROCESO | CANTIDADES |
| Materia prima inicial: Cáscara de | 5371 g |
| Peso de las cenizas después de | 567 g |
| Rendimiento de las cenizas | 10.56% |
| Cantidad de sílice obtenida | 100 g |
| Rendimiento de nanosílice | 2.79% |

Table 11

Nanosilica Production Cost.

| | | | | | |
|---|--|---|-------------------------------|---|-------------|
|  | | UNIVERSIDAD CENTRAL DEL ECUADOR FACULTAD DE INGENIERÍA Y CIENCIAS APLICADAS CARRERA DE INGENIERÍA CIVIL | |  | |
| Realizado por: | | Carlosama A. & Rosillo J. | | | |
| Proyecto: | | Síntesis de nano sílice a partir de la cáscara de avena para modificar las propiedades físicas y mecánicas del mortero con un enfoque eco amigable. | | | |
| ANÁLISIS DE PRECIOS UNITARIOS DE LAS MEZCLAS DE MORTERO | | | | | |
| Rubro: | | Síntesis de nanosílice de 100 gr | | | |
| Unidad: | | gr | | | |
| A. MATERIAL | | | | | |
| DESCRIPCIÓN | | UNIDAD | CANTIDAD | PRECIO UNITARIO | COSTO |
| Cáscara de avena | | kg | 5.37 | 0.50 | 2.69 |
| Ácido Sulfúrico | | L | 1.13 | 4.00 | 4.54 |
| Hidróxido de sodio | | kg | 1.13 | 3.00 | 3.40 |
| Agua destilada | | L | 80.00 | 0.50 | 40.00 |
| Energía eléctrica | | kW/h | 20.50 | 0.10 | 2.05 |
| SUBTOTAL | | | | | 52.67 |
| B. MANO DE OBRA | | | | | |
| DESCRIPCIÓN | | UNIDAD | Cantidad | Jornal (USD/hora) | COSTO |
| Técnico de laboratorio | | hora | 20.50 | 3.00 | 61.50 |
| Ayudante de laboratorio | | hora | 20.50 | 2.50 | 51.25 |
| SUBTOTAL | | | | | 112.75 |
| C. MATERIALES | | | | | |
| DESCRIPCIÓN | | UNIDAD | CANTIDAD | PRECIO UNITARIO (USD/h) | COSTO C=A*B |
| Horno de calcinación | | hora | 20.000 | 1.00 | 20.000 |
| Bomba de succión al vacío | | hora | 150.000 | 1.00 | 150.000 |
| SUBTOTAL | | | | | 170.00 |
| D. COSTO INDIRECTO | | | | | |
| DESCRIPCIÓN | | | CANTIDAD A | COSTO HORA | |
| | | | 10% | 33.542 | |
| SUBTOTAL | | | | 33.54 | |
| NOTA: ESTOS PRECIOS NO INCLUYEN EL IVA | | | TOTAL COSTO DIRECTO (A+B+C+D) | | |
| | | | COSTO INDIRECTO | | |
| | | | COSTO TOTAL DEL RUBRO: (USD) | | |
| | | | 368.97 | | |
| | | | 0 | | |
| | | | 368.97 | | |